Title

Ab initio study of enhanced thermal conductivity in ordered AlGaO3 alloys

Journal

Applied Physics Letters, 115(24)

ISSN

0003-6951

Authors

Mu, Sai
Peelaers, Hartwin
Van de Walle, Chris G

Publication Date

2019-12-09

DOI

10.1063/1.5131755

Peer reviewed

Applied Physics Letters

Ab initio study of enhanced thermal conductivity in ordered $AlGaO_3$ alloys

Cite as: Appl. Phys. Lett. **115**, 242103 (2019); https://doi.org/10.1063/1.5131755
Submitted: 15 October 2019 . Accepted: 03 December 2019 . Published Online: 12 December 2019

Sai Mu, Hartwin Peelaers, and Chris G. Van de Walle

AIP Publishing

Applied Physics Letters ARTICLE scitation.org/journal/apl

Ab initio study of enhanced thermal conductivity in ordered $AlGaO_3$ alloys

Cite as: Appl. Phys. Lett. **115**, 242103 (2019); doi: 10.1063/1.5131755
Submitted: 15 October 2019 · Accepted: 3 December 2019 ·
Published Online: 12 December 2019

Sai Mu,[1] Hartwin Peelaers,[2] and Chris G. Van de Walle[1,a)]

AFFILIATIONS

[1]Materials Department, University of California, Santa Barbara, California 93106, USA
[2]Department of Physics and Astronomy, University of Kansas, Lawrence, Kansas 66045, USA

[a)]Electronic mail: vandewal@ucsb.edu

ABSTRACT

We compute the lattice thermal conductivity of monoclinic β-Ga_2O_3 and the ordered $AlGaO_3$ alloy from the phonon Boltzmann transport equation, with the harmonic and third-order anharmonic force constants calculated from density functional theory. The calculated thermal conductivity of β-Ga_2O_3 is consistent with experiment. We demonstrate that the lowest-energy structure of an $Al_{0.5}Ga_{0.5}$ alloy, which is ordered, has a thermal conductivity that is raised by more than 70% compared to β-Ga_2O_3. We attribute the enhancement to (1) increased group velocities and (2) reduced anharmonic scattering rates due to the reduced weighted phase space. The findings offer an avenue toward improved heat dissipation from Ga_2O_3 devices.

Gallium oxide (Ga_2O_3) is a unique material with many promising applications in high-power and high-frequency electronics.[1] The large bandgap (4.76 eV, Refs. 2 and 3) of the monoclinic β-phase of Ga_2O_3 (hereafter denoted as β-Ga_2O_3) leads to a high breakdown field (6–8 MV/cm).[4] In spite of its large bandgap, Ga_2O_3 can be easily *n*-type doped.[4,5] These superior properties, combined with the availability of high-quality substrates,[6] render Ga_2O_3 a promising candidate for a new class of electronic devices.

Alloying can be used to modify the structural and electronic properties of Ga_2O_3. Alloying with In_2O_3 lowers the bandgap,[7] while adding Al increases the gap.[8] β-$(Al_xGa_{1-x})_2O_3/Ga_2O_3$ heterostructures that allow modulation doping and the formation of a two-dimensional electron gas (2DEG) have been demonstrated.[9,10] In spite of the promising applications, the low thermal conductivity of Ga_2O_3 ($\sim$20 W/mK)[11–13] is still a potential show-stopper. An increase in device temperature lowers the electron mobility, and limited heat dissipation will impact the performance and reliability of high-power devices. The low thermal conductivity can be attributed to the low-symmetry monoclinic crystal structure of β-Ga_2O_3, which leads to many phonon branches and thus an enlarged phase space for phonon scattering. This problem is aggravated in heterostructures, since alloying causes increased phonon scattering resulting from disorder.[14] In semiconductors, the thermal conductivity as a function of alloy concentration typically exhibits a *U* shape: the thermal conductivity is high for the end compounds and rapidly declines upon alloying. This has been observed for disordered alloys such as $Si_{1-x}Ge_x$, $In_xGa_{1-x}As$, and $Al_xGa_{1-x}As$.[15]

Disorder in the alloy is the main reason for the rapid decline in thermal conductivity. This raises the question whether ordered alloys might offer an opportunity to improve the lattice thermal conductivity. The monoclinic structure has equal numbers of four-fold- and sixfold-coordinated cation sites. A recent first-principles study demonstrated that in $Al_xGa_{1-x}O_3$ alloys, Ga can incorporate on either site but Al has a strong preference for the sixfold (octahedral) sites.[8] At 50% Al concentration, a highly stable ordered alloy ($AlGaO_3$) forms in which all Al atoms occupy octahedral sites[8] [see the inset of Fig. 1(a)]. In the present study, we employ density functional theory combined with the Boltzmann transport equation (BTE) to investigate the lattice thermal conductivity of ordered $AlGaO_3$. We also perform calculations for β-Ga_2O_3 for purposes of comparison and benchmarking.

The density functional calculations were performed using projector augmented wave (PAW)[16] potentials as implemented in the Vienna *Ab initio* Simulation Package (VASP),[17,18] with a 500 eV kinetic energy cutoff in the plane wave expansion. The PAW pseudopotentials correspond to the valence-electron configuration $3d^{10}4s^24p^1$ for Ga, $3s^23p^1$ for Al, and $2s^22p^4$ for O. The exchange-correlation is treated in the generalized gradient approximation, parameterized by Perdew, Burke, and Ernzerhof (PBE).[19] The Ga_2O_3 and ordered $AlGaO_3$ bulk structures were calculated using the 10-atom primitive

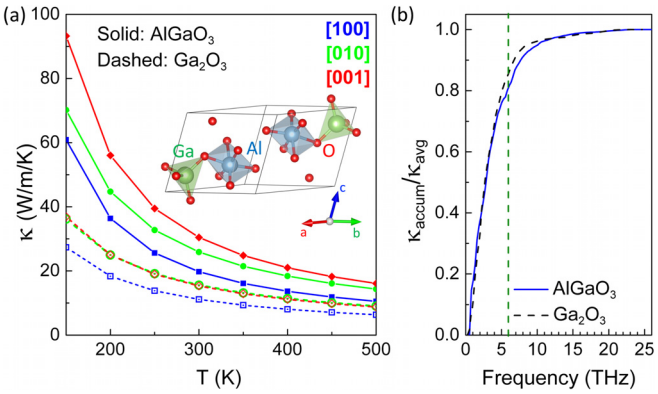

FIG. 1. (a) Calculated lattice thermal conductivity of Ga_2O_3 (dashed lines) and $AlGaO_3$ (solid lines). Colors describe thermal transport along different directions: [100] (blue squares), [010] (green circles), and [001] (red diamonds). The inset depicts the crystal structure of $AlGaO_3$. O, Ga, and Al atoms are represented by red, green, and blue spheres, respectively. (b) Room-temperature (normalized) accumulative averaged thermal conductivity as a function of frequency for Ga_2O_3 (dashed lines) and $AlGaO_3$ (solid lines).

cell and an $8 \times 8 \times 8$ k-point grid. Full relaxations were performed with Hellmann-Feynman forces converged to 0.005 eV/Å.

Interatomic force constants (IFCs) were calculated using the finite-displacement method in a $2 \times 2 \times 2$ (80-atom) supercell with a $4 \times 4 \times 4$ k-point grid. The harmonic IFCs give rise to phonon dispersion, while third-order anharmonic IFCs lead to scattering as a result of three-phonon interactions. Interactions up to the third-nearest neighbor were employed for the anharmonic IFCs, while harmonic IFCs were determined for all interactions within the supercell. The phonon scattering rates and lattice thermal conductivity were calculated using the ShengBTE package,[20] which solves the BTE iteratively.[21] The thermal conductivity tensor is given by

$$\kappa^{\alpha\beta}(T) = \frac{1}{V}\sum_{\lambda} C_{\lambda}(T)\nu_{\lambda}^{\alpha}\nu_{\lambda}^{\beta}\tau_{\lambda}(T), \quad (1)$$

where $\lambda = (n, \mathbf{q})$ labels the phonon branch n and the wave vector $\mathbf{q}$, and α, β are Cartesian coordinates. V is the cell volume, $C_{\lambda}(T)$ is the temperature-dependent specific heat, ν_{λ} is the group velocity, and τ_{λ} is the phonon lifetime, defined as the inverse of the phonon scattering rate. Only the dominant three-phonon scattering process has been considered. An $11 \times 11 \times 11$ q-point grid was employed to converge the room-temperature thermal conductivity; q-point convergence tests are included in the supplementary material (Sec. S1). The effect of the nonanalytical correction[22] on both the phonon bands (calculated using Phonopy[23]) and the resulting thermal conductivity has been included.

β-Ga_2O_3 has the monoclinic space group (C2/m). In the primitive (10-atom) unit cell, two of the Ga atoms occupy tetrahedral sites, and the other two atoms occupy octahedral sites. The ordered $AlGaO_3$ alloy maintains the same primitive cell and space group, with Al occupying the octahedral sites. The optimized lattice parameters for Ga_2O_3 and $AlGaO_3$ are listed in Table I. The calculated lattice parameters of Ga_2O_3 are slightly overestimated (by 1.3%–1.7%) compared with experiment.[24] We have checked that uncertainty in lattice parameters affects the thermal conductivity values by less than 16% and does not impact any of our conclusions. The inclusion of Al, which has a smaller atomic size than Ga, leads to a reduction in the volume of the primitive cell from 109.88 Å^3 for Ga_2O_3 to 101.98 Å^3 for $AlGaO_3$.

TABLE I. Structural information (lattice parameters, Å; angle β, °; volume of the 10-atom primitive cell V, Å^3), average atomic mass (M_{avg}, amu), room-temperature specific heat C_v (J/K mol, normalized to one mole of atoms), room-temperature thermal conductivity (κ, W/mK), and acoustic phonon group velocity (sound velocity) (ν, km/s) along [100], [010], [001] directions for Ga_2O_3 and $AlGaO_3$. For Ga_2O_3, experimental results are also listed for comparison.

	Ga_2O_3		$AlGaO_3$
	Calc	Expt	Calc
a	12.44	12.21[a]	12.16
b	3.08	3.04[a]	2.99
c	5.88	5.80[a]	5.78
β	103.28	103.83[a]	103.84
V	109.88	104.52[a]	101.98
M_{avg}	37.5		28.9
C_v	18.9	18.6[b]	17.7
$\kappa_{[100]}$	11.1(16.1[c])	11.0[b], 14.8[d]	19.8
$\kappa_{[010]}$	15.5 (21.5[c])	26.8[b],19.5[e]	25.0
$\kappa_{[001]}$	15.3 (21.2[c])	14.6[b]	30.4
$\nu_{[100]}$	LA: 7.3; TA: 2.3–3.5		LA: 8.4; TA: 3.2–4.4
$\nu_{[010]}$	LA: 7.3; TA: 2.4–3.5		LA: 8.5; TA: 3.2–4.4
$\nu_{[001]}$	LA: 7.8; TA: 2.9–3.3		LA: 9.5; TA: 3.5–4.1

[a]Reference 24.
[b]Reference 11.
[c]Reference 25.
[d]Reference 13.
[e]Reference 12.

The preference of Al atoms for octahedral sites was first revealed by hybrid functional calculations;[8] here, we found the same result based on PBE calculations. In the $AlGaO_3$ structure, the total energy for Al occupying octahedral sites is 120 meV/(formula unit) (PBE) or 140 meV/f.u. (hybrid functional) lower than that for Al occupying tetrahedral sites. The same conclusion applies to an alloy with 25% Al concentration (i.e., one Al per 4-cation primitive cell): octahedral sites are still preferred by Al atoms, and the energy penalty for Al occupying tetrahedral sites is 62 meV/f.u. (PBE) or 70 meV/f.u. (hybrid functional).

We investigated the possibility of site disorder by calculating the energy cost for swapping Al and Ga atoms. We performed these calculations in an 80-atom supercell of the ordered $AlGaO_3$ alloy. Regardless of the distance between the swapped Al and Ga atoms, the energy cost was found be to greater than 0.17 eV. This reinforces the notion of the octahedral-site preference of Al and indicates that site disorder on the cation lattice will be a minor issue in the ordered $AlGaO_3$ alloy.

The site preference correlates with the preferred coordination environment of Al vs Ga: Al atoms always favor octahedral positions (cf. the coordination of the cation sites in corundum). We found that in order to obtain these results, it is essential to include Ga 3d electrons in the valence states. If the d electrons are treated as part of the core in the PAW potential, Al atoms prefer to incorporate on tetrahedral sites

(with an energy gain of 50 meV/f.u. compared to Al on octahedral sites). We also find that treating d electrons as part of the valence is essential for obtaining the correct energetic ordering for the phases of Ga_2O_3 (monoclinic being lower in energy than corundum). We attribute the importance of Ga 3d states to the fact that they are close in energy to the O s states; the resulting hybridization impacts the energetics, as also observed by Sabino *et al.*[26]

Our calculated κ values along three crystallographic directions are shown in Fig. 1(a) as a function of temperature. In space group C2/m, the only nonzero components of a second-rank 3×3 tensor such as $\hat{\kappa}$ are κ_{xx}, κ_{yy}, κ_{zz} and $\kappa_{xz} = \kappa_{zx}$. κ values along the [100], [010], [001] directions are projected from the κ tensor in Cartesian coordinates as detailed in Sec. S2 of the supplementary material. The calculated room-temperature values are listed in Table I. Strong anisotropy is evident for both Ga_2O_3 and $AlGaO_3$.

The thermal conductivity of bulk β-Ga_2O_3 has previously been investigated theoretically by Santia *et al.*[25] and also in several experiments.[11–13] As seen in Table I, our calculated values generally compare well with experiments (a comparison of the temperature-dependent κ with experiments is shown in Sec. S3 of the supplementary material). A disagreement occurs with the experimental value of $\kappa_{[010]}$ from Guo *et al.*,[11] but we note that value differs significantly from the value reported by Galazka *et al.*[12] As to the comparison with the calculations of Ref. 25, we suggest that the difference can be attributed to the methodology: if Ga 3d orbitals are excluded from the valence states, κ values increase by 3–4 W/mK (see Sec. S4 of the supplementary material).

Turning now to $AlGaO_3$, Fig. 1(a) shows a sizable enhancement of $\hat{\kappa}$ for $AlGaO_3$ compared to Ga_2O_3 over the entire temperature range. At 300 K, κ is increased by as much as 70%–100% (see Table I). The enhancement can be understood based on the empirical rules outlined by Slack,[27] who attributed higher thermal conductivity to (1) lighter average atomic mass (M_{avg}); (2) stronger interatomic bonding; (3) simpler crystal structure with higher symmetry; and/or (4) decreased anharmonicity. In the present case, M_{avg} is reduced by 23% in the 50% Al alloy [rule (1)]. The $AlGaO_3$ alloy also displays stronger interatomic bonding [rule (2)], as evidenced by the bond-stretching IFCs for Al-O bonds being about 10% higher than for Ga-O bonds. As shown in detail below, the combined effect of reduced M_{avg} [rule (1)] and stronger interatomic bonding [rule (2)] leads to an increase in the sound velocities (Table I) that enter the expression for κ [Eq. (1)]. Our detailed analysis will also show that alloying does not result in a decrease in anharmonic force constants [rule (4)]; instead, the enhanced κ of $AlGaO_3$ is related to a decrease in the number of potential phonon scattering events.

To gain further insights into the enhancement of the thermal conductivity, we now examine the factors that enter Eq. (1). The volume is reduced in going from Ga_2O_3 to $AlGaO_3$, which is in principle favorable. However, the calculated specific heat (C_v) is also slightly reduced (see Table I), and the reduction in C_v almost exactly cancels the increase in $1/V$, leading to almost no change in κ. Thus, the enhancement of thermal conductivity must be ascribed to the other two factors in Eq. (1): the group velocities and the scattering rates.

Group velocities are determined by phonon dispersion. Figure 2 compares the phonon band structures for Ga_2O_3 and $AlGaO_3$; the high-symmetry points of the Brillouin zone for monoclinic β-Ga_2O_3 were identified in Ref. 28. Because of the low symmetry of the monoclinic structure, with 10 atoms in the primitive cell, the phonon band

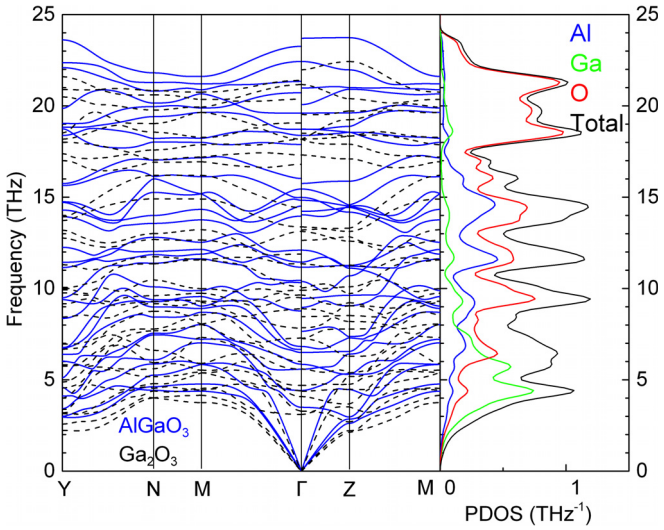

FIG. 2. Left panel: calculated phonon dispersion of Ga_2O_3 (black dashed lines) and $AlGaO_3$ (blue solid lines). Right panel: species-projected phonon density of states (PDOS, in THz^{-1} per f.u.) for Al (blue), Ga (green), O (red), and total (black) in $AlGaO_3$.

structure contains 30 branches. Fortunately, it is justified to focus on a subset of these modes. Figure 1(b) shows the accumulative averaged thermal conductivity (κ_{accum}) normalized by the total average thermal conductivity (defined as $\kappa_{avg} = \mathrm{Tr}[\hat{\kappa}]/3$) at room temperature as a function of frequency for Ga_2O_3 and $AlGaO_3$. $\kappa_{accum}/\kappa_{avg}$ gives the integrated contributions for all the phonon modes up to a certain frequency. For both materials, 80% of the thermal conductivity can be attributed to phonon modes with frequencies up to 6 THz. We therefore focus our discussion on this low-frequency region.

The frequency region up to 6 THz is dominated by the three acoustic modes, but these modes mix with low-frequency optical modes. These optical phonons provide additional scattering channels for the heat-carrying acoustic modes, effectively reducing the thermal conductivity. The calculated κ_{avg} of β-Ga_2O_3 is only 14 W/mK, an order of magnitude smaller than κ of wurtzite GaN (220 W/mK, Ref. 29), another wide-band-gap semiconductor that is being developed for high-power devices. The larger κ of GaN can be attributed to the acoustic and optical phonon bands being separated by a large gap, which quenches the scattering of acoustic phonons by optical phonons.[30]

In the right panel of Fig. 2, we project the phonon density of states (PDOS) of $AlGaO_3$ on different species. The heat-carrying low-frequency phonon modes are mainly associated with the heavy Ga atoms, while the high-frequency modes are dominated by the light O atoms. Substituting Ga with Al causes all phonon branches to move toward higher frequencies, due to the lighter atomic mass and larger force constants. One may expect that this increase in frequency also leads to larger group velocities. Indeed, inspection of $v_\lambda^\alpha v_\lambda^\beta$ [which enters Eq. (1)] indicates an increase in going from Ga_2O_3 to $AlGaO_3$ (see the plot in Sec. S5 of the supplementary material), thus contributing to an enhancement in κ.

We now discuss the final factor in Eq. (1), namely, the anharmonic three-phonon scattering rates ($1/\tau$). The room-temperature rates for Ga_2O_3 and $AlGaO_3$ are plotted in Fig. 3(a), focusing on the

low frequencies that are most relevant for κ. The scattering rates for Ga_2O_3 are clearly higher than for $AlGaO_3$, leading to a lower κ of Ga_2O_3. The scattering rates stem from a combined effect of the anharmonicity (third-order anharmonic IFCs) and the weighted phase space (solely determined by harmonic IFCs). The weighted phase space, as defined in Ref. 31 (see also Sec. S6 of the supplementary material), measures the number of three-phonon scattering processes that satisfy energy and momentum conservation. In order to distinguish between these effects, we recalculated κ of Ga_2O_3 but with the anharmonic IFCs of $AlGaO_3$. The κ tensor barely changes (Sec. S7 of the supplementary material). This result allows us to conclude that it is not the magnitude of the anharmonic IFCs that is driving the enhancement of κ in $AlGaO_3$, but rather the effect of the weighted phase space.

Indeed, Fig. 3(b) shows that the weighted phase space is a lot lower in $AlGaO_3$ than in Ga_2O_3, explaining most of the difference in scattering rates [Fig. 3(a)]. The difference in weighted phase space can be attributed to specific features in the phonon dispersion. As seen in Fig. 3(c), the low-frequency optical modes of Ga_2O_3 are lower in frequency than those of $AlGaO_3$, and thus, they interact more strongly with the heat-carrying acoustic modes. This leads to more "avoided crossings" in the phonon branches in Ga_2O_3 than in $AlGaO_3$, as highlighted in Fig. 3(c). Avoided crossings are typical indicators of strong acoustic-optical phonon coupling, which is known to reduce the thermal conductivity.[31,32]

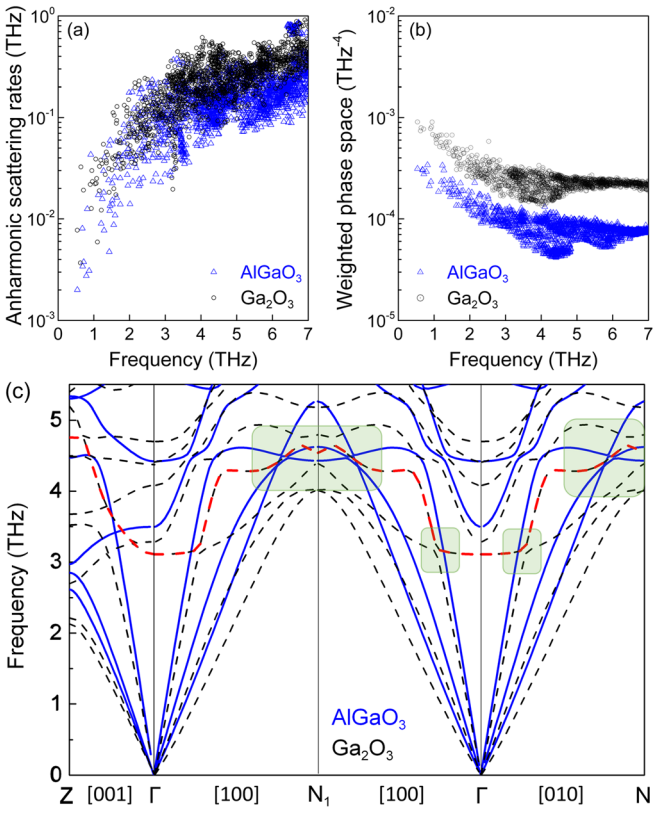

FIG. 3. (a) Calculated anharmonic scattering rates and (b) weighted phase space, as a function of frequency for Ga_2O_3 (black circles) and $AlGaO_3$ (blue triangles) at room temperature. (c) Low-frequency phonon bands of Ga_2O_3 (black dashed line) and $AlGaO_3$ (blue solid line) along [001], [100] and [010] directions. The red dashed line depicts a low-frequency optical mode of Ga_2O_3 that interacts with the acoustic modes. The avoided-crossing features in Ga_2O_3 phonon bands are highlighted using shaded areas.

We have demonstrated that substituting light Al atoms on cation sites in Ga_2O_3 leads to enhanced κ. However, it requires the formation of an ordered structure to avoid phonon scattering due to alloy disorder. Long-range ordering has been observed in alloyed semiconductor thin films, such as $Al_xGa_{1-x}N$[33] and $Ga_xIn_{1-x}P$.[34] These precedents strengthen the prospects for experimental synthesis of ordered $AlGaO_3/Ga_2O_3$ thin films.

In conclusion, based on first-principles calculations and Boltzmann transport simulations, we have shown that alloying Ga_2O_3 with 50% Al—forming an ordered alloy—increases the components of the thermal conductivity tensor by 70%–100%. We attributed the enhancement to a reduction in mass and increase in bond strength, which lead to higher group velocities, and to a reduction in overlap between acoustic and low-frequency optical modes, which leads to a decrease in scattering processes. The prospect of enhanced thermal conductivity will hopefully stimulate experimental efforts to grow the ordered $AlGaO_3$ structure.

See the supplementary material for the q-point convergence tests, relation between crystallographic and Cartesian directions, comparison with temperature-dependent experimental data, impact of Ga 3*d* orbitals, comparison of group velocities, definition of weighted phase space, and impact of anharmonic IFCs.

The authors acknowledge Shengying Yue, Jingjing Shi, Samuel Graham, and Yuewei Zhang for fruitful discussions. This work was supported by the GAME MURI of the Air Force Office of Scientific Research (No. FA9550-18-1-0479). Computing resources were provided by the Center for Scientific Computing supported by the California NanoSystems Institute and the Materials Research Science and Engineering Center (MRSEC) at UC Santa Barbara through the National Science Foundation (NSF) (Nos. DMR-1720256 and CNS-1725797) and by the Extreme Science and Engineering Discovery Environment (XSEDE), which was supported by NSF Grant No. ACI-1548562.

REFERENCES

[1]M. Higashiwaki and G. H. Jessen, Appl. Phys. Lett. **112**, 060401 (2018).
[2]H. Tippins, Phys. Rev. **140**, A316 (1965).
[3]T. Matsumoto, M. Aoki, A. Kinoshita, and T. Aono, Jpn. J. Appl. Phys., Part 1 **13**, 1578 (1974).
[4]M. Higashiwaki, K. Sasaki, A. Kuramata, T. Masui, and S. Yamakoshi, Appl. Phys. Lett. **100**, 013504 (2012).
[5]J. B. Varley, J. R. Weber, A. Janotti, and C. G. Van de Walle, Appl. Phys. Lett. **97**, 142106 (2010).
[6]E. G. Víllora, K. Shimamura, Y. Yoshikawa, K. Aoki, and N. Ichinose, J. Cryst. Growth **270**, 420 (2004).
[7]H. Peelaers, D. Steiauf, J. B. Varley, A. Janotti, and C. G. Van de Walle, Phys. Rev. B **92**, 085206 (2015).
[8]H. Peelaers, J. B. Varley, J. S. Speck, and C. G. Van de Walle, Appl. Phys. Lett. **112**, 242101 (2018).
[9]E. Ahmadi, O. S. Koksaldi, X. Zheng, T. Mates, Y. Oshima, U. K. Mishra, and J. S. Speck, Appl. Phys. Express **10**, 071101 (2017).
[10]Y. Zhang, A. Neal, Z. Xia, C. Joishi, J. M. Johnson, Y. Zheng, S. Bajaj, M. Brenner, D. Dorsey, K. Chabak *et al.*, Appl. Phys. Lett. **112**, 173502 (2018).

[11]Z. Guo, A. Verma, X. Wu, F. Sun, A. Hickman, T. Masui, A. Kuramata, M. Higashiwaki, D. Jena, and T. Luo, Appl. Phys. Lett. **106**, 111909 (2015).
[12]Z. Galazka, K. Irmscher, R. Uecker, R. Bertram, M. Pietsch, A. Kwasniewski, M. Naumann, T. Schulz, R. Schewski, D. Klimm *et al.*, J. Cryst. Growth **404**, 184 (2014).
[13]M. Handwerg, R. Mitdank, Z. Galazka, and S. F. Fischer, Semicond. Sci. Technol. **30**, 024006 (2015).
[14]P. Klemens, Proc. Phys. Soc. **68**, 1113 (1955).
[15]P. Maycock, Solid State Electron. **10**, 161 (1967).
[16]P. E. Blöchl, Phys. Rev. B **50**, 17953 (1994).
[17]G. Kresse and J. Hafner, Phys. Rev. B **48**, 13115 (1993).
[18]G. Kresse and J. Furthmüller, Phys. Rev. B **54**, 11169 (1996).
[19]J. Perdew, K. Burke, and M. Ernzerhof, Phys. Rev. Lett. **77**, 3865 (1996).
[20]W. Li, J. Carrete, N. A. Katcho, and N. Mingo, Comput. Phys. Commun. **185**, 1747 (2014).
[21]M. Omini and A. Sparavigna, Phys. Rev. B **53**, 9064 (1996).
[22]X. Gonze and C. Lee, Phys. Rev. B **55**, 10355 (1997).
[23]A. Togo and I. Tanaka, Scr. Mater. **108**, 1 (2015).
[24]J. Åhman, G. Svensson, and J. Albertsson, Acta Crystallogr., Sect. C **52**, 1336 (1996).
[25]M. D. Santia, N. Tandon, and J. Albrecht, Appl. Phys. Lett. **107**, 041907 (2015).
[26]F. P. Sabino, L. N. de Oliveira, and J. L. Da Silva, Phys. Rev. B **90**, 155206 (2014).
[27]G. A. Slack, J. Phys. Chem. Solids **34**, 321 (1973).
[28]H. Peelaers and C. G. Van de Walle, Phys. Status Solidi B **252**, 828 (2015).
[29]A. Jeżowski, B. Danilchenko, M. Boćkowski, I. Grzegory, S. Krukowski, T. Suski, and T. Paszkiewicz, Solid State Commun. **128**, 69 (2003).
[30]L. Lindsay, D. Broido, and T. Reinecke, Phys. Rev. Lett. **109**, 095901 (2012).
[31]W. Li and N. Mingo, Phys. Rev. B **91**, 144304 (2015).
[32]O. Delaire, J. Ma, K. Marty, A. F. May, M. A. McGuire, M.-H. Du, D. J. Singh, A. Podlesnyak, G. Ehlers, M. Lumsden *et al.*, Nat. Mater. **10**, 614 (2011).
[33]D. Korakakis, K. Ludwig, Jr., and T. Moustakas, Appl. Phys. Lett. **71**, 72 (1997).
[34]A. Gomyo, T. Suzuki, and S. Iijima, Phys. Rev. Lett. **60**, 2645 (1988).